

Resource Management for Fault Tolerant Path Structures in SONET Ring Networks

Wayne D. Grover^{1,2}

There is growing interest on the part of network operators in the ability to analyze the availability of path implementations in their networks and to provide various grades of assured service availability to customers. The calculation of availability is, however, considerably more complex in today's SONET ring-based networks than in prior point-to-point systems. This is due both to the active protection nature of the rings and their dual-redundant interconnect strategies. We show that there is also more than one option for dual-ring interconnection and that a minimum cost high availability path implementation will generally involve a mixture of matched-node and explicitly dual fed treatments. We develop an economic comparison of dual feeding (*df*) and matched nodes (*mn*) in terms of the resource consumption of each scheme and show that the choice can be made on an individual ring-by-ring basis with a simple decision criterion. We then develop expressions of general use for the end-to-end unavailability of single-fed, pure *df*, *mn* and mixed *df-mn* path constructions. These results are a step towards on-line provisioning or path planning systems that can minimize the path implementation cost subject to an assured target level of design availability.

KEY WORDS: Fault tolerance; survivable networks; self-healing rings; matched nodes; dual ring interconnect; availability.

1. INTRODUCTION

1.1. Background and Objectives

Customers more and more expect that network operators provide service contracts with assured availability objectives, and corresponding rebates or penalties if the targets are not met. For instance, a service agreement may guarantee a month without charge if there is more than a minute of outage in the

¹TR Labs and Department of Electrical and Computer Engineering, University of Alberta, Edmonton, Canada.

²To whom correspondence should be addressed at TR Labs, #800 10611-98 Ave., Edmonton, Alberta, Canada T5K 2P7. E-mail: grover@trlabs.ca

preceding month. SONET rings [1–4] are one of the transport technologies that are allowing operators to achieve high service availability. When a transport signal is in the body of a ring, it is protected by the reverse-direction routing mechanism. A more difficult and costly issue for network operators is, however, whether or not to provide dual-redundant *inter-ring* connections when implementing some or all paths in their network. It would obviously be of value to a telco to know if single feeding was fully adequate to meet availability objectives for a given service path. Considerable cost for extra add-drop interfaces and bandwidth consumption is saved if dual ring interconnect is not needed. On the other hand it is also important to know when redundant inter-ring connections will be required to meet availability objectives and, in this case, to know the lowest cost strategy for redundant interconnection. We will show this involves a ring-by-ring decision between either matched nodes with a drop-and-continue arrangement, or use of explicit dual feeding strategies, to be defined.

The paper makes several contributions to assist network operators in facing these issues. First, we show that dual feeding can be a more cost effective alternative to matched nodes in a fairly wide range of applications. This is a simple, useful, but not so obvious, option for telcos to be aware of in path provisioning. Second, we provide exact analytical results for the two-failure outage of line-switched rings due to node or link failure within the ring, for both single and dual feeding cases. In doing so we also point out the applicability to unidirectional path switched rings. A final contribution is to extend the availability results to provide a means of exact calculation of end-to-end availability for paths implemented over several concatenated rings where the inter-ring treatments may be based on any mixture of dual-feeding and matched-node arrangements. The calculation of availability of heterogeneous redundant path constructions through ring-based networks is a step towards an automated path provisioning system which will synthesize the route and path construction details that minimize implementation cost subject to a guaranteed design availability target. The issues addressed in this paper are limited in scope to policies surrounding the provisioning of new paths for service growth and rearrangements within an existing design of rings and gateway nodes. In this context the set of available rings and gateway node locations is given and common to all alternatives. The full network design problem, which is to determine the placement of rings and gateway nodes in the first place, is not the purpose of this work. However insights on availability-driven provisioning strategies given a set of rings can be a factor influencing the design problem itself.

1.2. Related Literature

This work involves the availability analysis of various SONET ring-to-ring interconnection schemes. We therefore review some relevant literature on these two aspects. To and Nuesy [5] have considered the availability of SONET and DS3

point-to-point systems, and certain digital cross-connect restoration schemes over a ladder-type hypothetical reference path. They derive results for 2-fiber and 4-fiber BLSRs, but do not consider the interconnection issues in a chain of rings. Their analytical method and assumptions are, however, the same as we use. To *et al.* [6] also use these methods to compare the availability of 2-fiber and 4-fiber BLSRs. Nagaraj *et al.* [7] provide a comparative study of the impact of SONET technology on network availability, relative to the preceding DS3-based transport era. They do not develop analytical results, but provide an example of the comparison of schemes on a hypothetical reference path model, again with the same working assumptions as To and Neusy [5]. Wilson [8] has similar comparisons of 2- and 4-fiber rings but does not present analytical formulations and does not consider the range of ring interconnection models that are covered here.

Regarding strategies for ring interconnection, Doshi *et al.* [9] have recently considered problems of ring exhaustion that arise in the conventional “matched node” method for dual ring interconnection, when the ‘continue’ spans become highly unbalanced. The alternatives they develop remain based on the drop-and-continue concept, but with extension to a three-node crossing arrangement over which the continue span loads can be better balanced. The alternative which we introduce is that of explicitly copying and dual feeding the payload signal over the interconnecting rings. It is not obvious, starting out, that such a simple but apparently extravagant measure could require fewer resources in some cases than the drop and continue method for dual ring interconnect.

Earlier related work by the author [10] considers pure dual-fed or pure matched-node path types, not the mixed *mn-df* constructions and *mn-df* decision criterion now considered for cost-optimal path construction. Access costs were also included in this work [10] but are excluded here because the access architecture is independent of the intra-ring routing choices. Grover [10] does, however, contain a more extensive tutorial review of SONET rings, network reliability, and availability analysis methods in general and, as such, may be a useful supplement to the present paper. The basic framework for cost and path availability analysis established [10] is re-used here, as is certain basic material required to make the present paper suitably self-contained.³ Other papers addressing current approaches and issues of fault tolerance in modern communication networks can be found in Medhi and Tipper [11].

1.3. Outline of Remaining Developments

We proceed as follows: The rest of Section 1 explains what we mean by the “matched nodes” (*mn*) and “dual-feeding” (*df*) arrangements for inter-ring

³Sections 2.1–2.3 and 3.1–3.3. These sections are essential background for the new results in 2.4 and 3.5.

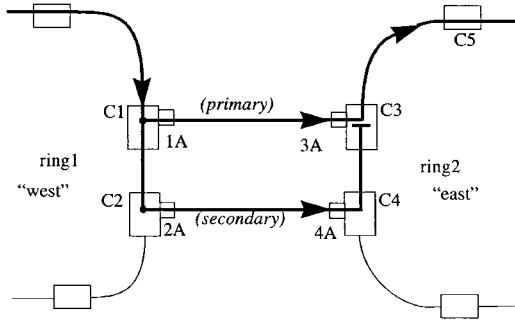


Fig. 1. Matched node drop and continue inter-ring transfer arrangement.

connection. Section 2 develops an economic criterion for the choice between *df* or *mn* treatment in any given ring. Section 3 is concerned with calculating the unavailability of path constructions of pure *df* rings, pure *mn* rings and of path constructions with mixed *df-mn* treatments along the end-to-end route of a path. The unavailability analysis complements the economic criterion for ring-by-ring choice by ensuring that the availability implications of these economic path constructions can be assessed. Section 4 summarizes.

1.4. Matched Nodes and "Drop-and-continue"

Bidirectional line-switched rings (BLSR) are widely used for implementing broadband SONET transport networks. When a transport signal, an STS-1 for example, is in the body of a BLSR it is protected against any single node or link failure by the reverse-direction routing mechanism of the BLSR [1, 2]. Therefore, two or more simultaneous failures are required to cause *intra-ring* outage. But if no special measures are taken, there will be a single point of failure at each site where *inter-ring* transfers occur. This may be acceptable for some traffic given that the transfer occurs in an inside-plant central office (C.O.) environment and that the cross-office wiring (or fibering) may itself be 1 + 1 protected. However, some customer leased signals, and/or special services signals may warrant routing and provisioning that avoids any single points of failure. For these signals, the "matched node"⁴ arrangement in Fig. 1 has been used widely by SONET ring network planners to date [1-4].

In a matched node (*mn*) arrangement, the service path transfers redundantly via two matched (also called gateway) nodes using the drop and continue feature

⁴The industry uses a variety of terms for this technique. "Matched nodes" tends to be used by one major supplier and its customers, whereas standards bodies tend use simply "drop and continue" and other suppliers use "dual-ring inter-working".

of SONET add drop multiplexers (ADMs). In Fig. 1 labels C1 through C4 designate the ADM cores involved in the redundant signal transfer and labels 1A to 4A designate the add/drop interfaces involved. Nodes C1 and C3 (similarly C2, C4) are usually in the same office and the low speed add/drop ports are interconnected by short- or medium- reach intra-office fiber cabling. The signal flow is drawn in a unidirectional manner but the complementary treatment for the opposite signal direction is implied. The transferring signal enters the primary gateway node C1 where it is dropped to C3, and is continued on ring 1 to the secondary node C2. The drop signal at C1 is supplied via a cross-office link to the primary destination gateway C3 for a standard tributary insertion (add). The continue signal in ring 1 is terminated at C2, dropped, and then added to the node C4. The primary gateway C3 on the destination ring thereby receives two copies of the transferring signal and performs 1 + 1 receive selection. This transfer arrangement is resilient to failure of any one of the four ADM cores or add/drop interfaces.

Less obviously, it also protects against total loss of either gateway site (e.g., loss of both nodes C1 and C3, or C2 and C4) and resists some other dual-failure combinations as well. To appreciate the latter, one must consider the ordinary line-level reverse direction routing reactions of rings 1 and 2 simultaneously with the tributary-level signal selection behavior. For instance, if the building housing C1 and C3 fails entirely (from, say, a fire or power loss) the tributary signal in ring 1 will be reverse routed onto protection (as part of the OC-n line level reaction in ring 1) to C2 where C2 will substitute the protection signal for the normal signal from C1. The secondary transfer path then conveys the tributary to C4. But C4 is also in loopback mode in response to loss of node C3. And C5, in ring 2, is also in loopback mode. The tributary is therefore reverse routed on protection bandwidth to C5 in ring 2, from where it resumes its normal routing.

1.5. The Dual-Feeding (df) Alternative

We will return to the matched node arrangement to study its 2-failure unavailability and its resource consumption costs. Presently, we wish to introduce the idea of direct dual feeding (*df*) of a signal as an alternative to matched nodes. Figure 2 shows how redundant inter-ring signal transfer can be achieved by establishing two physically identifiable copies of the signal in the two rings, with direct transfers at the same two crossing points as in Fig. 1.

In Fig. 2 there are no drop and continue signal arrangements, nor 1 + 1 selection sites to support the transfer function. The payload signal is itself simply duplicated in each ring and transfers directly across at the gateway node pairs. Clearly, this may consume more bandwidth in the rings than the *mn* setup because the latter has only one ‘working’ path within each ring. On the other hand, the dual feeding setup requires no ‘continue’ bandwidth, so we should not rule out either *df* and *mn* approaches *a priori*. ADM core bandwidth use, add-drop interface use and ‘con-

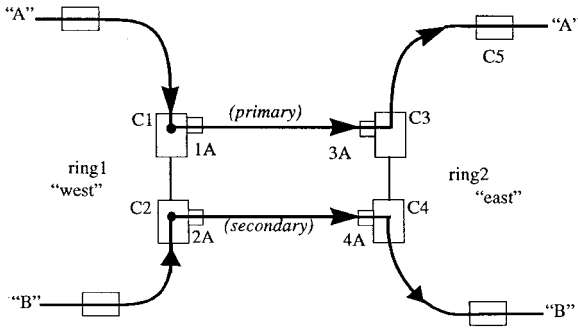


Fig. 2. Dual feeding direct transfer inter-ring arrangement.

tinue' signal bandwidth consumption (and existing span utilization levels if near-exhaust conditions are involved) are all factors in determining which scheme will actually cost less (or delay span exhaustion) in a given situation.

1.6. Functional Compatibility of *mn* and *df* Treatments

Next, we want to establish that *df* and *mn* treatment can be determined and applied on a ring by ring basis. Consider the following assertions: (i) *mn* on a "West" ring is functionally compatible and can be directly interfaced to *df* in an adjoining "East" ring, and vice-versa; (ii) the *mn* or *df* decision can be made independently within each ring, based on the parameters of each ring alone. That is two (or more) rings do not need to be considered together to decide which treatment is most economical.

Point (i) is a simple observation that is illustrated in Fig. 3 by an example of an *mn*-to-*df* conversion, connecting successive rings in a signal path.

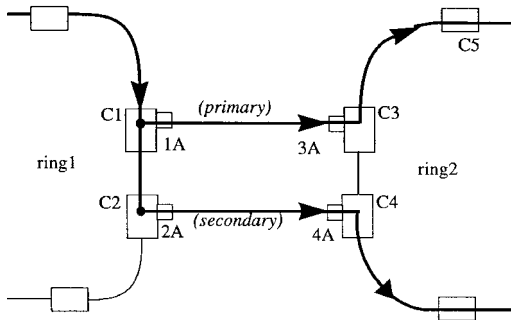


Fig. 3. Matched nodes (*mn*) in ring 1 with dual feeding (*df*) in ring 2.

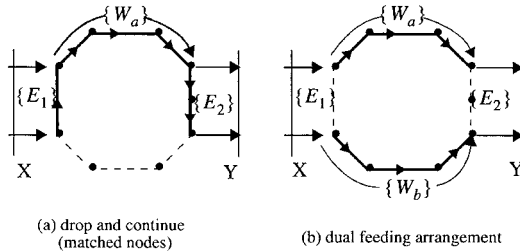


Fig. 4. Considerations for ring-by-ring choice between *mn* or *df*.

Point (ii) is a less obvious claim. It says that, from an economic viewpoint, we can choose the treatment independently in each ring and the resulting complete path will be cost minimal; i.e., that the sum of the economically best treatments in each ring is globally the best treatment for this problem. (The path unavailability implications will not have a similar independence property and are assessed later.)

To explain this point regarding economic optimization of the path, consider Fig. 4. In Fig. 4, the *mn* and *df* approaches are illustrated at a whole-ring level showing the signal routing that each scheme implies within the ring. In a ring configured for *mn* style redundant interfaces, the working signal is physically present only on the $\{E1, Wa, E2\}$ path shown. Regarding notation, we use $\{-\}$ to denote a set of elements. Thus, Wa and S are just scalars (numbers of spans) whereas $\{Wa\}$ is the set of all elements (OC-n line km, ADM nodes, optical interfaces etc.) in the specified path segment. Wa is the number of spans along the working path between the primary matched nodes. $E1$ and $E2$ are the number of spans between redundant entry and exit node locations, respectively. We consider general values of $E1$ and $E2$ but most often in practice today $E1 = E2 = 1$. Figure 4b shows the dual fed alternative at the same whole-ring level. $\{Wa\}$ is the same as in *mn*. $\{Wb\}$ is the path of the explicit additional signal feed that is required in the *df* approach.

Clearly, the two approaches are functionally equivalent if viewed through interfaces X and Y . There is no observation at interface Y (other than possibly some long term difference in unavailability) that would allow one to tell the difference between (a) and (b) in Fig. 4. Therefore (a) and (b) must be functionally interchangeable with regard to interface Y . But the same arguments apply to the prior ring at the interface X . Therefore we are free to choose between *mn* or *df* independently within each ring, because the signal arrangement in one ring has no functional influence or dependence on the configuration in an adjacent ring. While the unavailability of the complete path construction will indeed depend on the ring-by-ring choices, and multi-ring sequence effects, it follows from this that from an economic decision viewpoint we can also optimize the treatment in each ring individually.

2. ECONOMIC DECISION CRITERION

2.1. Framework for Resource Cost Assessment

For generality, we take an approach that avoids dependence on specific cost data. We formulate the comparative cost of *mn* and *df* treatments in terms of the weighted conversion of equipment items and other resources into a resource consumption function that is used as a surrogate for cost. Three cost characteristics are considered: distance-dependent transmission costs, ADM core costs, and tributary-related ADM interface costs. Figure 5 helps explain the variables in the resource cost assessment of alternatives.

The pro-rated cost of passing one tributary signal unit through one ADM chassis is defined as the fundamental “unit cost” (1.0). The “tributary signal unit” is the smallest unit of bandwidth under management for provisioning, i.e., STS-1 if STS-1, STS-3 or STS-12 paths can be provisioned. (In this way the decision framework is simply repeated and scaled in any context such as if DS1 were the basic provisioning unit or entire STS-48 wavelengths will be the provisioning bandwidth unit in dense WDM.) An ADM core or “chassis” refers to all the common equipment infrastructure (card cage, backplane, power, control processors, plus East and West dual optical line interfaces) of the ADM before any tributary cards are added. Relative to this unit cost, β is defined as the cost of an add/drop interface for one signal unit, and α is the relative cost of a unit distance of intra-ring optical line transport at the respective tributary bandwidth being considered. α and β are both pro-rated to the ADM core transit cost on a unit bandwidth basis. This may not always be apparent for the optical line cost factor (α) because the line OC-n rate is normally the same as the ADM backplane bandwidth, so α is also the ratio of the whole optical line cost (per km) to the whole ADM chassis cost. In other words $\alpha = \text{transport cost per bandwidth unit-distance} / \text{chassis cost per unit bandwidth}$, which also equals $\text{OC-n cost per unit distance} / \text{total OC-n chassis cost}$.

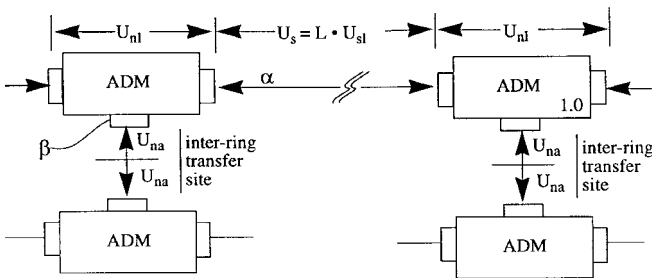


Fig. 5. Elemental unavailability and resource cost models for ring network elements.

Using α and β as study parameters for comparative assessment of alternatives we can obtain general conclusions without dependence on specific cost data. These parameters also define a parameter space which can systematically represent variations in geographic scale, and the effects of a variety of technology assumptions. For instance, in metropolitan networks, spans often do not require regenerators and previously placed dark fiber is available in existing ducts. Consequently distance-related transmission costs are often treated as negligible, and the planning problem reduces to minimizing the terminal equipment cost. This is the $\alpha = \text{zero}$ situation in our framework. On the other hand, in a long-haul network, the cost of the transmission systems may be greater than the nodal terminal costs, in which case α has a more significant numerical effect reflecting the cost of a OC- n line systems relative to the OC- n ADM chassis cost. The influence of α is therefore related to geographical network scale. On the other hand β , is more likely to depend on the technology epoch assumed. To illustrate, imagine an STS-3c add/drop interface circuit pack to have a fixed absolute cost and imagine this unit being used interchangeably for STS-3c applications on an existing OC-48 ADM and on a newer OC-192 ADM. For illustration only, assume the more advanced ADM core costs the same as its OC-48 predecessor. In a study with the OC-192 ADM's, β would then be 4 times higher (i.e., when normalized to the core chassis cost per bandwidth unit) than in the same study assuming the OC-48 ADM, (both routing STS-3c paths), because while the cost of the add-drop interface is the same, the fraction of the nodal core cost on a unit bandwidth basis is four times lower with the OC-192. This framework is also used in [10] for comparative study of unavailability and cost in various end-to-end path models including access costs and access effects on path availability.

Note that this framework is an average-case allocation of relative resource costs. It takes the viewpoint of having to decide between provisioning policies for repeated application in a continually growing network context. The average-case cost allocation is reasonable as a method for comparative policy assessment, when instances of the same decision choice are faced repeatedly. Any one individual planning situation can, however, involve module-filling considerations due to the discrete modular nature of rings. For instance, if a ring has enough bandwidth on spans to support a *df* implementation, say, while the intra-ring 'continue' signal would saturate a span of the ring, then a specific case arises in which the average-case provisioning cost allocations do not really capture the nonlinearity involved if the *mn* choice would trigger a whole additional ring, but the *df* case would not. Therefore, while we use an average-case allocation of costs to seek generalized comparative insights about the merits of the various strategies, planners need also to recognize these case-specific effects when they are relevant and make more specific cost analyzes reflecting the nonlinear modularity effects, if continued regular growth throughout the next module is not anticipated. The example of premature

exhaustion of a ring from the accumulation of continue signals between gateway nodes is in fact a particularly well known “high penalty” case for which some alternatives other than dual feeding are studied [9].

2.2. Resource Cost for Matched Node Treatment

We consider the resource cost of the mn configuration in two steps: First we consider the ADM core consumption, add/drop interface consumption, and distance-bandwidth span consumption costs of the $\{W_a\}$ path through the ring between the primary matched nodes. Then we add considerations of the drop and continue setups at each side of the ring. Inside the ring on the $\{W_a\}$ signal path, there are W_a working spans and $W_a + 1$ nodes. However, the cores of the entry and egress ADMs on each ring are only “half-transited” by the tributary signal of interest. At the other ADMs in $\{W_a\}$ the core is fully traversed. The total ADM core consumption is therefore $W_a + 1 - 2(1/2) = W_a$ unit costs per ring. One add/drop interface is used on each side of the ring in $\{W_a\}$. W_a spans of line-level transport are used in each ring, where $L_s(i)$ will be the length of the i th span.

To add the matched node setup to the $\{W_a\}$ path, the ADM core consumption goes up by a $1/2$ core transit at the primary and secondary gateway nodes. That is, the continue signal completes a transit of the primary node cores and a half-transit is added at each secondary node. Additional whole core transits occur if either entry or egress separations are more than one span apart. In general $E - 1$ additional core transits and E spans for the continue signal are added to the $\{W_a\}$ path for each entry or egress separation of E . Finally, the drop and continue setup adds one more add/drop interface at each side of the ring. The resource cost of mn (in order of cores, spans, interfaces) is therefore:

$$C_{mn} = (W_a + E_1 + E_2) + \alpha \cdot \left(\sum_{i \in \{W_a, E_1, E_2\}} L_S[i] \right) + 4\beta \quad (2.1)$$

2.3. Resource Cost of the Dual-Fed Treatment

The corresponding resource cost for df is obtained from Fig. 4b as follows: The df path pair almost circumnavigates each ring. In total there are $W_a + W_b = (S - E_1 - E_2)$ spans traversed. S is the number of spans in a particular ring. All ADM cores on the $\{W_a\}$ or $\{W_b\}$ paths are fully traversed by either the “A” or “B” signal feed, but at the ends of each feed the respective signal copies only “half transit” the ADM core for a total ADM core consumption of $(S - E_1 - E_2)$ units of core ADM capacity. There are also 4 add/drop interfaces consumed. Therefore we can write:

$$C_{df} = (S - E_1 - E_2) + \alpha \cdot \left(\sum_{i \in \{W_a, W_b\}} L_S[i] \right) + 4\beta \tag{2.2}$$

2.4. Decision Criterion

By recognizing that $W_b = S - W_a - E_1 - E_2$, and that the number of add-drop interfaces, as well as $\{W_a\}$, is common to both Eqs. (2.1) and (2.2), we can form a decision variable ΔC :

$$\begin{aligned} \Delta C &\equiv (C_{mn} - C_{df}) \\ &= W_a + 2 \cdot (E_1 + E_2) - S + \alpha \cdot \left(\sum_{i \in \{E_1, E_2\}} L_S[i] - \sum_{i \in \{W_b\}} L_S[i] \right) \end{aligned} \tag{2.3}$$

If ΔC is positive, the *df* treatment is more cost effective than using matched nodes. To understand the factors affecting the *df-mn* criterion further, let us consider the special case where all spans are of equal length (or cost) L_S . Then the *mn-df* cost difference simplifies to:

$$\Delta C = [W_a + 2 \cdot (E_1 + E_2) - S] \cdot (1 + \alpha \cdot L_S) \tag{2.4}$$

The criterion simplifies to this form because, with the half-transit considerations for entry and egress ADM cores, the number of spans traversed is numerically equal to the number of core bandwidth units used. Each span costs αL_S and, by definition, each unit of core bandwidth costs 1.0.

As seems reasonable from Fig. 4, Eq. (2.4) tells us that large rings (large in number of spans S) favor the matched node treatment. This is offset in favor of dual feeding, however, if the entry and egress separation sum $E_{tot} = (E_1 + E_2)$ is large or if the $\{W_a\}$ path is long.

While ΔC is the actual cost difference, if we are interested only in a binary *mn* versus *df* decision criteria, then we can further reduce this to:

$$W_a \geq S - 2 \cdot E_{tot} \rightarrow df, \quad \text{otherwise } mn \tag{2.5a}$$

or equivalently,

$$W_b \leq E_{tot} \rightarrow df, \quad \text{otherwise } mn \tag{2.5b}$$

as a criterion for triggering the *df* approach rather than *mn*. Of course in applying

Eq. (2.5) the minimum value for E_{tot} is 2. $W_a > 0$ is also required. Similarly the minimum size ring for the df versus mn comparison to be meaningful is at $S=4$.

Although it is trivial to mechanize Eq. (2.5), doing so demonstrates that there is a considerable scope for df applications. Fig. 6(a) is from a spreadsheet where the criterion is applied at every valid (i.e., feasible to construct) point in the application space of rings from 4 to 16 spans and for E_{tot} from 2 to 14 spans. Figure 6a is also generated for a specific, fairly conservative, assumption about the length of the shortest working path through the ring (i.e., W_a) in terms of the ring size. This is, for purposes of this illustration only, that W_a spans only 1/4 of the ring after excluding the entry and egress separations. Of course this "1/4 rule" is conditioned to nonzero integer values. Even with this conservative assumption about W_a , Fig. 6a shows that df would be equal or lower in cost in over half the points in the complete application space. In practice today, most applications may be on the lower half of the E_{tot} axis, favoring mn . Nonetheless the applications range for df is not insignificant in Fig. 6a. It may also be expected that once df is more widely understood as a provisioning option, the wide egress routing choices which are only really feasible with df , and which favor df economics, may become more common. Figure 6b is the corresponding decision space outcomes where W_a is larger, nominally half of the ring size, after excluding entry/egress spans. This is the more optimistic, but not unrealistic, case for df and a very significant application range is now seen for df in Fig. 6b.

Strictly speaking, $\Delta C = 0$ implies a 'tie' between mn and df (the circle symbols in Fig. 6). However, it may in practice be considered as a case where df is preferred because, if all else is equal, df eliminates the matched node 1 + 1 select function and is also generally easier to establish, operate, and manage, than mn . Additionally, a mixture of mn and df treatments for various paths through the same gateway node pairs will help keep span bandwidths more balanced. Note also that in developing the decision criterion we have assumed that the crossing locations used for dual feeding are the same as would be used for matched node pairs. This may not always be the case in practise: It is easy for a df path pair to have any E separation whereas it is operationally more complex to establish and operate multi-hop continue signal arrangements for the mn alternative. This is an additional unquantified factor in favor of the df option. Comparing the two with identical crossing points is actually generous towards mn because it does not penalize mn in any extra way for the considerable practical difficulties of *extended* (i.e., multi-span) continue signals.

3. PATH UNAVAILABILITY ANALYSES

We now give consideration to the calculation of end-to-end path availability of the pure df , pure mn and mixed df - mn path constructions that may result

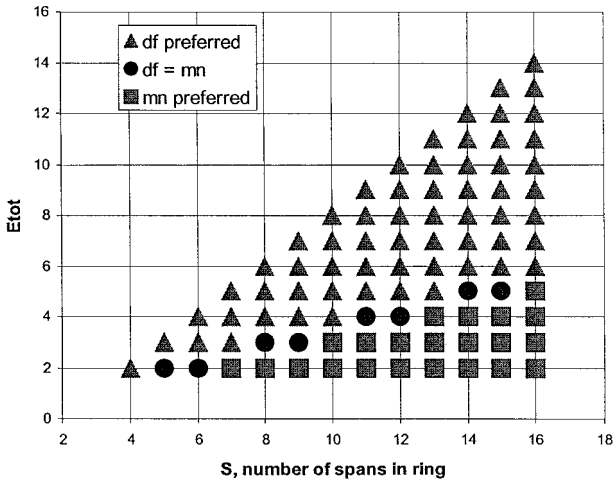
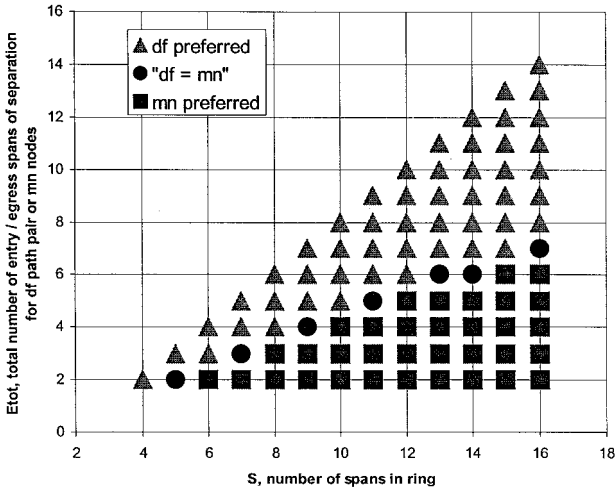


Fig. 6. Outcome of *df-mn* decision criterion for (top) $W_a = \max(\text{floor}(S - E_{tot})/4, 1)$, and (bottom) $W_a = \max(\text{floor}(S - E_{tot})/2, 1)$.

from the application of a ring-by-ring *df-versus-mn* decision criterion. We proceed by first considering the 2-failure *intra-ring* outage contributions from each ring in the path depending on its internal configuration. Then we consider the dual-failure combinations that cause outage due to element failures in the *inter-ring* transfer interfaces. Standard methods and assumptions for the availability

of repairable, actively maintained, systems are used [12]. The elemental unavailability variables are illustrated in Fig. 5. U_{sl} is the unavailability per km of optical line length excluding ADM nodes and ADM optical interfaces. Span unavailability $U_s = U_{sl} * L_s$ is used directly (i.e., as U_s) in the following, where L_s is the length of a fiber span in a BLSR but more generally U_s can be comprised of a weighted sum of distances and transmission-type specific unavailabilities per km. U_{nl} is the unavailability of a tributary signal path through the ADM core. It includes optical interfaces, but no add/drop interfaces. U_{na} is the unavailability of the add/drop interface and half of any cross-office connection path for a tributary signal to transit from one ring to another. While we will use equal length spans for illustrative comparative purposes, it is understood that users can apply the actual distances and unavailability data per mile that applies to their specific path models.

3.1. Intra-Ring Dual Failure Transport Outage Contributions

In this section we develop the expressions $Td_1(W, S)$ and $Td_2(W, S, E)$ for the *intra-ring* contributions to path unavailability with a single-fed path and a dual-fed signal path, respectively, through a BLSR. This is a step towards calculating the unavailability of multi-ring paths of *mn*, *df* and *mn-df* mixed constructions. The “*d*” in Td_1 , Td_2 is used to designate a dual-failure analysis. The 1,2, subscripts denote whether a single or dual signal instance physically traverses the ring in question. Thus $Td_1()$ will be applicable to rings in *mn* configuration and $Td_2()$ to *df* rings. $Td_1()$ and $Td_2()$ functions include the optical line side signal path failures at the primary entry and egress nodes, and the ADM cores, but not the add/drop side (or tributary-level) failures at these nodes or failures involving the drop and continue setups for *mn*. The latter are accounted for in the *inter-ring* transfer terms of the path-level models that follow.

$Td_1(W, S)$ is the line-level intra-ring transport unavailability of a single-fed signal path traversing W spans of a BLSR having S spans in total. It accounts for all statistically independent double-failure event combinations with consideration of the line-switched protection mechanism. $Td_1(W, S)$ is derived as follows: Let the set of W spans and $(W+1)$ nodes in the normal path of a signal feed X through a ring be called the *forward path of X*, denoted $For\{X\}$ where $\{-\}$ denotes a set. Let the set of all other nodes and spans in the ring be $Rev\{X\}$. i.e., $Rev\{X\} = \{S\} - For\{X\}$ where $\{S\}$ is the complete ring. $Rev\{X\}$ has $S-W$ spans. For outage of a single-fed path within a ring, it is necessary, and sufficient, that one failed element (node or span) belong to $For\{X\}$ and the other to $Rev\{X\}$. The relevant pairs consist of: a span in $For\{X\}$ and a span in $Rev\{X\}$, a span in $For\{X\}$ and a node in $Rev\{X\}$ or *vice versa*, and a node in $For\{X\}$ and a node in $Rev\{X\}$. Triple and higher multiplicity failure combinations are ignored. Summing and simplifying all contributions we obtain:

$$T_{d1}[W, S] = W(S - W)Us^2 + (W + 1)(S - W - 1)Unl^2 + (2W(S - W - 1) + S) \cdot UsUnl \tag{3.1}$$

This result is essentially the same as for the corresponding case in (see To and Neusy [5]). Although this work is primarily devoted to considering BLSRs, it can be shown that the $Td1()$ function above also applies identically to unidirectional path-switched (UPSR) rings, because the 1 + 1 UPSR working signal copies circumnavigate the ring, just as do the working and protect paths in BLSR. The failure scenarios and combinations reflected in $Td1()$ consequently turn out to be identical in the UPSR.

A slightly different function, $Td2()$, is needed for the intra-ring transport unavailability of a BLSR where dual redundant signal feeds are explicitly provisioned through the BLSR. For a single-fed path, the forward path plus reverse path for line switched protection circumnavigates the whole ring, $|For\{X\}| + |Rev\{X\}| = S$. But when dual feeding, the relevant element subsets do not circumnavigate the ring. When dual feeding A and B paths, outage requires one failure in $\{For\{A\} AND Rev\{B\}\}$ and the other in $\{Rev\{A\}\} AND For\{B\}\}$. This is the only way two failures can be positioned so as to simultaneously fail A and B forward feeds and both of their respective line-switched restoration paths. However, because the A and B signal feeds are disjoint $\{Rev\{A\} AND For\{B\}\} = For\{B\}$ because $For\{B\}$ is necessarily a subset of the path $Rev\{A\}$. Likewise, $\{For\{A\} AND Rev\{B\}\} = For\{A\}$. Hence, outage simply requires one failure in $For\{A\}$ and one failure in $For\{B\}$ and there is no exposure to failures on spans or nodes not directly on one of the A/B feeding paths. For example, when a dual fed path pair enter and leave the ring one node apart, (i.e., $E_{tot} = 2$), $|For\{A\}| + |For\{B\}| = S - 2$, so there are two fewer spans to contribute to the failure combinations than with $Td1()$ for the A signal feed alone in the same ring. From these considerations, the dual-failure combinations that bring down both A & B feeds of a dual-fed path pair in a BLSR is obtained as:

$$T_{d2}[S, W_a, E_{tot}] = W_aW_bUs^2 + (W_a + 1)(W_b + 1)Unl^2 + (2W_aW_b + W_a + W_b)UsUnl \tag{3.2}$$

where $W_b = S - W_a - E_{tot}$ and W_a, S and E_{tot} are as before.⁵

An insight obtained from the process of developing these expressions is that dual-feeding through a BLSR does not radically improve the unavailability relative to single feeding because the state of the restoration path $Rev\{A\}$ for sig-

⁵Note: As written, Eqs. (3.1) and (3.2) apply for the case of all spans being of equal length. For varying span lengths replace W variables in the first and third terms by the actual sum of span lengths and replace U_S by U_{Sl} in those terms only.

nal feed A is highly correlated with events on the forward path of the (ideally independent) B feed, and *vice versa*. In other words, the explicitly duplicated signal feed plays a role that is almost, but not wholly, equivalent to the ordinary line protection mechanism in the sense that most of the 2-failure combinations that bring down $For\{X\}$ and $Rev\{X\}$ for the single fed case also simultaneously fail $For\{A\}$ and $For\{B\}$ in dual feeding. In contrast, dual feeding should be considered primarily for the economic benefit in suitable ring situations not for an intra-ring unavailability advantage. Dual feeding will also have some availability gain, however, to the extent that the overlap of $For\{B\}$ and $Rev\{A\}$ paths (and *vice versa*) is not complete; i.e., the $\{E1\} + \{E2\}$ sets are removed from the 2-failure outage combinations when dual feeding. The greatest intra-ring unavailability benefit from dual feeding is therefore when the sum of entry and exit node pair separations is large.

3.2. Unavailability of a Single—Fed (*sf*) Path

Single feeding (*sf*) is the least costly, but lowest availability path provisioning scheme. In *sf*, the signal path originates at the add side interface at a node on a first ring, traverses that ring via some working path $\{W\}$, then is dropped from the ring, transfers (cross-office) to the add side of another ring, and so on. The signal is protected enroute wherever it is inside a ring, but makes nonredundant inter-ring transfers. (Nonredundant in the sense that geographically distinct crossing points are not used. As mentioned, the single logical cross-office path between two *sf* rings may actually be 1 + 1 protected within the C.O. If so, this is reflected in the *Una* value to be used, not in the path-level routing model.) The simple series-element summation of the intra-ring and inter-ring unavailabilities in the path therefore gives the unavailability of an *sf* path through K rings:

$$U_{sf}[K] = 2K(U_{NA} + U_{NL}) + \sum_{i=1}^K T_{d1}[W_i, S_i] \quad (3.3)$$

3.3. Unavailability of a Pure Matched Node Path

It is clear from inspection of Fig. 1 that the matched node arrangement protects the inter-ring transfer against failure of any one of the four ADMs performing add/drop functions. As previously explained, however, it also makes the inter-ring transfer immune to total loss of either gateway *site* (e.g., both C1 and C3 or C2 and C4), due to combined actions of each BLSR and the matched node gateway select function. Through similar case-by-case, functional analysis, all possible 2-element failures in the matched node system have been considered for their outage-causing effects. The result is in Table I. The main finding is

that only simultaneous pairs of same-ring (e.g., C1, C2) or diagonal cross-ring (e.g., C1, C4) ADM core or add/drop interface failures can defeat the matched node arrangement. Simultaneous failure of both ADM cores on one side of the gateway is also outage causing, but it is separately accounted for in $Td_1()$, as a dual-failure *intra*-ring outage. Additionally, due to the line-level BLSR reaction, a span failure between the primary and secondary nodes on either ring and another single element failure in the inter-ring interface will not defeat the *mn* scheme. Such failures are isolated within their respective rings and have no opportunity to combine into an outage-causing dual failure. The remaining failure combinations are detailed in Table I. The result is that each inter-ring transfer in an *mn* path contributes $2U_{NL}^2 + 4U_{NA}^2 + 8U_{NL}U_{NA}$. Therefore, the overall unavailability of a redundant path construction which begins at the inputs to the add/drop interfaces on the redundant entry and egress nodes in the first and last rings and contains K rings all interconnected via matched nodes is:

$$U_{mn}[K] = 2(U_{NA}^2 + 2U_{NA}U_{NL}) + 2(K - 1)(U_{NL}^2 + 2U_{NA}^2 + 4U_{NA}U_{NL}) + \sum_{i=1}^K T_{d1}[W_i, S_i] \tag{3.4}$$

Table I. Dual-Failure Analysis for the *mn* Transfer Arrangement

Dual-element failure (Description)	Example of failure class	Unavailability (per individual combination)	No. of combinations
1. 2 ADM cores (nodes) on the same ring	C1-C2	covered by $Td_1()$	2
2. 2 ADM cores at opposite facing nodes	C1-C3	not outage causing	2
3. cores of diagonally opposite ADMs	C1-C4	U_{nl}^2	2
4. two add/drop I/Fs on different nodes of the same ring	1A-2A	U_{nl}^2	2
5. two add/drop I/Fs on diagonally opposite nodes	1A-4A	U_{na}^2	2
6. two add/drop I/Fs on facing opposite nodes	1A-3A	not outage causing	2
7. add/drop I/F at a node on ring 1 and ADM core loss at diagonally opposite node	1A-C4	$U_{na}U_{nl}$	4
8. core loss on one ring with add/drop I/F loss at other node on same ring	C1-2A	$U_{na}U_{nl}$	4
9. core loss and same-node add/drop I/F	C1-1A	not outage causing	4
10. core loss and add/drop I/F at facing node	C1-3A	not outage causing	4
		Total combinations	28

3.4. Unavailability of a Pure Dual-Fed Path

In dual feeding the separate A/B feeds make their way individually across the inter-ring interfaces, as in Fig. 2. At the first and last rings in this path model each signal feed is delivered from their separate ADM drop interfaces to the CPE location via a separate access link (i.e., if ring 1 in Fig. 2 (or in Fig. 7) was the last ring in the path, then the primary and secondary transfer signals shown go via access links to the CPE location.) Inside each ring, the *intra*-ring dual failure outage is accounted for by $T_{d2}()$ terms. Therefore, as in *mn*, single span or ADM node failures within a BLSR are isolated and do not accumulate in combinations end-to-end over the A/B paths. In a *df* path construction, however, one failure at *any inter-ring* transfer site on feed “A” can combine with a single failure at *any other* (or the same) transfer point on the “B” path causing outage. In fact the *df* path construction can be viewed as a parallel redundant pair of *sf* paths, except that each ring enroute is traversed in a dual feeding manner so the intra ring unavailability will be given by $T_{d2}()$ terms, rather than $T_{d1}()$. Regarding *inter-ring* failures, each constituent “A” or “B” *sf* signal feed has $2K$ add/drop interface points, which are independent of the opposite signal feed. At each of these interfaces, either an add/drop interface failure, or failure of the core of the ADM where the signal is entering a ring, can fail the individual path. The service path as a whole will fail if two failures combine within one ring, or if any inter-ring or entry/egress interface failure on one feed combines with a similar failure anywhere on the other signal feed. Thus, we would expect to have $\{2K(U_{NL} + U_{NA})\}^2$ contribution from all pairs of independent failures at ring entry or inter-transfer points on the path pair. This must be modified slightly, however, because the complete combinatorial pairing of events that this expresses includes a subset of same-ring dual-node failure pairs that can indeed fail the service at inter-ring transfer points, but which are already accounted for in the $T_{d2}()$ contributions. In other words we must remove $2KU_{NA}^2$ to avoid double-counting these particular failure combinations. The result is:

$$U_{df}(K) = 4K^2(U_{NL} + U_{NA})^2 - 2KU_{NL}^2 + \sum_{i=1}^K T_{d2}[W_{A_i}, S_i, E_i] \quad (3.5)$$

Note the trade-off that Eq. (3.5) expresses relative to that for the pure *mn* path, Eq. (3.4): $T_{d2}()$ terms are involved, rather than $T_{d1}()$ so the *intra*-ring availability is better than *mn*, but this is countered by a square law increase in outage due to inter-ring transfers in proportion to the logical length of the path (K), which is not present in *mn* path constructions.

3.5. Unavailability of a Mixed *df-mn* Path Constructions

In a mixed path implementation, as depicted in Fig. 7, the total path unavailability may be obtained by breaking the path into segments of rings that share the same routing strategy. Within these segments the unavailability can be calculated from Eqs. (3.4) and (3.5). However, the embedding of a *df* segment between *mn* segments introduces a class of outage-causing failure combinations that are not accounted for in the pure-*df* or *mn* segment models themselves. Consider *df* segment 1 in Fig. 7. Dual failures of add/drop interfaces and/or nodal cores at A, B or G, H cause outage, but are accounted for in the *mn* segment 1 and *mn* segment 2 models. The same combinations at nodes C, D or E, F and the cumulative nonisolated C, F or D, E type failures in *df* are similarly already accounted for in the *df* segment 1 model. But consider a single failure in *mn* ring 1, at node A, and in *mn* ring 4, at node H. Such failures, in separate *mn* rings, would not previously have been outage-causing as they would be isolated single failures in a pure-*mn* segment. But when they occur in combination, at the interfaces to the *df* segment, the failure at node A voids the *df* “A” feed entirely through *df* segment 1, and the failure at H prevents the surviving *df* “B” feed from getting into the next *mn* segment. This is a unique *mn-df-mn* combination that is not accounted for in any of the pure-segment models themselves. It adds $2U_{NA}^2 + 4U_{NA}U_{NL}$ for each *embedded df* segment, but does not exist for a nonembedded *df* segment, such as ring 6, that is at the outside of the path.

Next, if *mn* node A (core or add/drop interface) fails, then any single inter-ring failure on the *df* “B” feed is also a new outage-causing inter-segment failure combination. This will add $4(U_{NL} + U_{NA})(K_{df}[i] - 1)(2(U_{NL} + U_{NA}))$ for an embedded *df* segment because there are 4 *mn* nodes that have this cross relationship to one of the *df* “A” or “B” paths. The leading coefficient will be 2 for a nonembedded *df* segment. Single intra-ring failures on feeds of the *df* segment are isolated from this *mn* node cross dependency by the BLSR line mechanism. Overall the unavailability of a mixed path construction becomes:

$$\begin{aligned}
 U_{dfmn}[N_{df}, N_{mn}] = & \sum_{j=1}^{N_{mn}} U_{mn}[K_{mn}[j]] + \sum_{i=1}^{N_{df}} \{U_{df}[K_{df}[i]] + 2\delta_{df}[i](U_{NA}^2 \\
 & + 2U_{NA}U_{NL}) + 4(1 + \delta_{df}[i]) \cdot (K_{df}[i] - 1) \cdot (U_{NA} + U_{NL})^2\}
 \end{aligned}
 \tag{3.6}$$

where $U_{df}[\]$ and $U_{mn}[\]$ are given by Eqs. (3.5) and (3.4), respectively, and N_{df} and N_{mn} are the number of dual fed and matched node contiguous segments in the overall path. $K_{df}[i]$ is the number of rings in the *i*th *df* segment and $K_{mn}[j]$

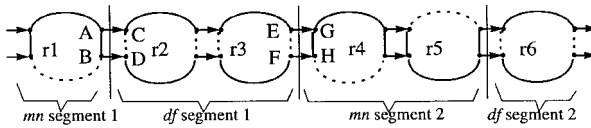


Fig. 7. Example of a mixed *df-mn* path construction: $N_{df} = N_{mn} = 2$; $K_{df}[i] = \{2, 1\}$; $K_{mn}[j] = \{1, 2\}$.

is the number of rings in the j th *mn* segment and $\delta_{df}[i] = 1$ if the i th *df* segment is embedded, otherwise $\delta_{df}[i] = 0$.

4. CONCLUSIONS

This work predicts economic benefits from considering the option of explicit dual feeding in some contexts where matched node arrangements would today be specified. The practical reason for dual feeding is not predominantly for its effect on intra-ring unavailability, although this is a positive effect. Rather, the more important motivation for dual feeding is that in some circumstances it can provide a lower cost means of *setting up for* a dual-redundant inter-ring transfer into the next ring. The extent to which dual feeding also improves the intra-ring service availability increases with E_{tot} , which is the total separation between entry and egress gateway node pairs. At small E_{tot} (2 or 3 say) there is little benefit—availability wise—from dual feeding because the basic (single-fed) BLSR mechanism is so similar in effect to dual feeding, in terms of the failure combinations covered. The *df* scheme does, however, eliminate the entry/egress spans from the failure combinations, thus improving availability as E_{tot} increases. Today, $E_{tot} = 2$ almost always in practice, because matched nodes virtually dictate $E_{tot} = 2$. This restriction, based on *mn* concept, however, should not be applied to assess the *df* benefit, because *df* is really free to use any E_{tot} . Based on the findings here, we encourage planners to consider *df* provisioning in situations that can explicitly take advantage of $E_{tot} > 2$ conditions. The difficulty that widely separated gateway locations causes in *mn* are just the situations that *df* can exploit to reduce cost and slightly improve availability at the same time. The *df* approach could also be usefully applied in practice when the *-mn* approach threatens to exhaust a ring on its continue spans or is causing low overall ring utilization due to continue signal accumulation effects as described in [9].

A relatively simple economic decision criterion for *mn* versus *df* was also given which applies on a ring-by-ring basis. The simplicity and ring-independence of this criterion is desirable in itself, but it implies that the min-cost end to end path constructions will, in general, be of a mixed *df-mn* construction. Therefore, we also provided a complete analytical model, built up from $Tdl()$,

$Td2()$ for intra ring effects, then up to K-ring pure $-mn$ or $-df$ segment effects, and finally representing complete heterogeneous paths of concatenated $-mn$ and $-df$ path segments, for the end-to-end availability of a generalized $-mn$ and $-df$ 'economic' path constructions.

In the long run, the ability to construct the min-cost path, and to compute its design availability right at provisioning time, would seem desirable in an online provisioning system. Minimum cost provisioning decisions could be made to support the availability-grade of the particular services being supported. This could provide significant savings compared to a policy using drop and continue in all cases. For certain services, or for short paths, pure sf (at roughly half the cost of either $-mn$ or $-df$) may be adequate, but this is only known if the path availability is calculated in conjunction with the provisioning details, at provisioning time. In other cases, calculations as given can show when df has lower cost than mn in cases where high availability (i.e., dual-ring interconnected) treatment is required. An eventual aim, advanced by this work, is to support a future online provisioning system which can synthesize the globally minimum cost path implementation that meets a contracted customer level of design availability.

REFERENCES

1. T.-H. Wu, *Fiber Network Service Survivability*, Artech House, Boston, Massachusetts, pp. 123–134; 439–441, 1992.
2. T. Flanagan, Fiber network survivability, *IEEE Communications Magazine*, Vol. 28, No. 6, June, pp. 46–53, 1990.
3. Nortel (Northern Telecom), *Introduction to SONET Networking*, October 1996: (available at <http://www.nortel.com/broadband>).
4. G. W. Ester, SONET: Interconnecting rings using drop and continue, *Telephone Engineer and Management*, June 1, 1993.
5. M. To and P. Neusy, Unavailability analysis of long-haul networks, *IEEE Journal on Selected Areas in Communications*, Vol. 12, No. 1, pp. 100–109, January 1994.
6. M. To, J. McEachern, and G. Copley, Unavailability analysis of 2 vs 4-fiber bi-directional rings, Rep. T1X1.5/91-159, October 1991.
7. K. Nagaraj, J. Gruber, J. Leeson, and B. Fleury, Improvements in availability and error performance of SONET compared to asynchronous transport systems. In C. A. Siller, M. Shafi (eds.), *SONET/SDH: A Sourcebook of Synchronous Networking*, IEEE Press, pp. 211–217, 1996.
8. M. R. Wilson, The quantitative impact of network survivability on service availabilities, *Proc. 12th Annual National Fiber Optics Engineers Conference*, Denver, pp. 919–930, September 1996.
9. B. T. Doshi, S. Dravida, P. Harshavardhana, P. K. Johri, and R. Nagarajan, Dual (SONET) ring interworking: High penalty cases and how to avoid them, *Proc. of ITC-15*, Washington, D.C., Elsevier, pp. 361–370, June 1997.
10. W. D. Grover, High availability path design in optical ring-based networks, *IEEE/ACM Trans. Networking*, Vol. 7, No. 4, pp. 558–574, August 1999.
11. D. Medhi and D. Tipper (eds.), Special issue: Fault management in communication networks, *Journal of Network and Systems Management*, Vol. 5, No. 2, pp. 101–215, June 1997.

12. R. Billinton and R. N. Allan, *Reliability Evaluation of Engineering Systems: Concepts and Techniques*, Second Edition, Plenum Press, 1992.

Wayne Grover obtained his B.Eng. from Carleton University, and M.Sc. from the University of Essex, and Ph.D. from the University of Alberta, all in Electrical Engineering. He had 10 years experience as scientific staff and management at BNR (now Nortel Technologies) before joining *TRLabs* as its founding Technical VP in 1986. He is now Chief Scientist—Network Systems, at *TRLabs* and Professor, Electrical and Computer Engineering, at the University of Alberta with research interests in SONET and ATM survivable ring, mesh and hybrid network operation and optimal design. He has patents issued on 17 topics to date, and in 1996 he received the *TRLabs* Technology Commercialization Award for the licensing of restoration-related technologies to industry.